

Titanian chondrodite- and titanian clinohumite-bearing metadunite from the 3800 Ma Isua supracrustal belt, West Greenland: Chemistry, petrology, and origin

ROBERT F. DYMEK

Department of Earth and Planetary Sciences and McDonnell Center for the Space Sciences,
Washington University, St. Louis, Missouri 63130, U.S.A.

JEREMY L. BOAK

ARCO Oil and Gas Company, P.O. Box 147, Bakersfield, California 93302, U.S.A.

SARA C. BROTHERS

Department of Geology, University of New Mexico, Albuquerque, New Mexico 87131, U.S.A.

ABSTRACT

Titanian chondrodite (Ti-Ch) and clinohumite (Ti-Cl) have been discovered in a serpentinite from the 3.8 Ga Isua supracrustal belt, West Greenland, where they occur with olivine ($\approx \text{Fo}_{97}$), magnesite ($X_{\text{Mg}} \approx 0.99$), magnetite, and Ni-Co-Pb sulfides in a matrix of antigorite. This serpentinite has the bulk composition of a dunite (Niggli value $mg \approx 0.89$), with high Ni (~ 2300 ppm) and Cr (~ 950 ppm), and its REE pattern is broadly similar to those reported for cumulate dunites of igneous origin. The highly magnesian phase compositions indicate that the metadunite evolved from a serpentinite precursor, which experienced additional late serpentinization. Two different generations of olivine and antigorite, both with slightly different compositions, indicate an extremely complex history for the sample. However, the titanian humites locally occur as inclusions in olivine, indicating that they formed relatively early.

Ti-Ch (~ 9 wt% TiO_2) occurs as separate grains and also forms lamellar intergrowths with Ti-Cl (~ 6 wt% TiO_2). These phases differ significantly only in terms of Ti/Si, as X_{Mg} (~ 0.98), X_{Ni} , X_{Mn} , X_{Ti} (~ 0.45), and X_{F} (~ 0.05) are similar. The high content of Ti and low content of F indicate nearly complete $\text{TiO}_2\text{Mg}_{-1}\text{F}_{-2}$ exchange, whereas the high X_{Mg} values make these the most magnesian Ti-rich humites yet reported.

The two-phase intergrowths may represent the reaction $\text{Ti-Ch} + \text{forsterite} = \text{Ti-Cl}$. The sample lacks geikielite or any magnesian ilmenite, indicating that the terminal breakdown of titanian humites by the reaction $\text{titanian humites} = \text{forsterite} + \text{geikielite} + \text{H}_2\text{O}$ was not approached. Chemographic relations for the system $\text{MgTiO}_3\text{-Mg}_2\text{SiO}_4\text{-H}_2\text{O}$ reveal that Ti-Ch should be the high-pressure humite phase, on account of the experimentally determined location of the Ti-Cl breakdown reaction (Engi and Lindsley, 1980).

The only other known occurrence of a Ti-Ch and Ti-Cl intergrowth is in kimberlite (Aoki et al., 1976), and the possibility that Ti-Ch is a mantle phase should be reconsidered. However, we do not regard the Isua sample to be of mantle origin, although the intergrowths may record decompression during the polymetamorphic history of the region.

INTRODUCTION

Natural occurrences of titanian clinohumite (Ti-Cl) are rare but have attracted considerable attention in recent years because they are found principally in ultramafic rocks, some of which are demonstrably of mantle origin. McGetchin et al. (1970) noted the presence of Ti-Cl in ultramafic nodules found in kimberlite from the Colorado Plateau and speculated that this phase could represent an important upper-mantle reservoir for volatiles, especially water. A number of reports have also described occurrences of Ti-Cl in peridotites and serpentinites from orogenic belts that include the Alps, the Apennines, and

the Ruby Range, Montana (e.g., Cimmino et al., 1979; Trommsdorff and Evans, 1980; Desmarais, 1981; Evans and Trommsdorff, 1983). The work of Trommsdorff and Evans (1980) is particularly important since it seems to establish on petrographic grounds that the stability field for Ti-Cl is contained fully within that of antigorite. Experimental work (Engi and Lindsley, 1980) has shown that Ti-Cl is unstable above 475°C at 3.5 kbar and 675°C at 21 kbar, which places severe limitations on the importance of this mineral to mantle petrology, while at the same time confirming its stability within the P - T regime relevant to "ordinary" crustal metamorphism.

TABLE 1. Chemical composition of Isua metadunite IW809-4

wt%		Cation %	
SiO ₂	41.30	Si	34.0
TiO ₂	0.09	Ti	0.1
Al ₂ O ₃	0.82	Al	0.8
FeO	9.92	Fe	6.8
MnO	0.16	Mn	0.1
MgO	47.07	Mg	57.8
CaO	0.25	Ca	0.2
Na ₂ O	0.06	Na	0.1
K ₂ O	0.07	K	<0.1
P ₂ O ₅	<0.03	P	<0.1
LOI	10.77		
ppm			
V	14	Rb	<1
Cr	958	Sr	<2
Ni	2357	Y	<1
Zn	59	Zr	<2
Ga	<1	Nb	<1
		Ba	<5
		Pb	13
		Th	<1
		Ce	0.925
		Nd	0.615
		Sm	0.143
		Eu	0.019
		Gd	0.171
		Dy	0.181
		Er	0.145
		Yb	0.196
Niggli value <i>mg</i> = 0.894		(Mg + Fe)/Si = 1.903	

Titanian chondrodite (Ti-Ch) is even more rare. Trommsdorff and Evans (1980) remarked upon its presence in their Alpine samples as a possible breakdown product of Ti-Cl. The only published analyses that we are aware of are those from the Buell Park, Arizona, kimberlite (Aoki et al., 1976; cf. Smith, 1977; Fujino and Takéuchi, 1978), where the Ti-Ch forms intergrowths with Ti-Cl. The exact paragenesis of this occurrence is unclear, as the humites were not recognized "in situ" but were recovered through mineral separation on crushed rock fragments.

In the course of investigating ultramafic metamorphic rocks from the 3.8 Ga Isua supracrustal belt, West Greenland, we have discovered Ti-Ch in a serpentinized metadunite, where it occurs as independent grains and also forms intergrowths with Ti-Cl. The purpose of this paper is to document the chemistry of these humites and to evaluate their petrogenesis in light of available data on other occurrences. The present paper follows upon preliminary results reported earlier (Dymek et al., 1983) and is expanded here to include a thorough account on the phase petrology of the host metadunite, together with additional information on its major- and trace-element composition.

GEOLOGIC SETTING AND SAMPLE DESCRIPTION

The Isua supracrustal belt (lat 65°15'N; long 50°00'W) is located in the central part of the West Greenland Archean gneiss complex. The geology of the Isua area has been studied by, among others, Bridgwater and McGregor (1974), Allaart (1976), and Nutman et al. (1984), who recognized a diverse suite of clastic and chemical metasedimentary rocks, mafic metavolcanic rocks, and stratiform ultramafic rocks. Various radiometric dating techniques have yielded ages for the supracrustal rocks in the 3700–3800 Ma range [see Baadsgaard et al. (1984) for recent summary], which leave little doubt as to the an-

tiquity of the Isua belt and establish it as the oldest dated group of rocks on Earth.

A variety of ultramafic rocks are found at Isua, including (1) massive metaperidotite-metadunite (olivine + chlorite + Cr-rich magnetite ± tremolite ± cumingtonite or anthophyllite ± dolomite ± magnesite, with relict green spinel + orthopyroxene found at one locality; Brothers and Dymek, 1983); (2) ultramafic schist derived from metaperidotite (talc + magnesite ± anthophyllite ± antigorite, with rare multiple chain silicates; O'Leary and Dymek, 1987); and, (3) antigorite serpentinite. Late lizardite and/or chrysotile, either as pseudomorphs after olivine or in small veins, occur in many samples.

The sample of interest here (IW809-4) is a serpentinite, having the bulk composition of a dunite (see below). It is fine-grained, dense, and very fresh, with the typical blue-gray color of the other Isua ultramafic rocks. IW809-4 was collected from one of a series of red-weathering outcrops that locally contain bladed (metamorphic) olivine crystals up to several centimeters long. These ultramafic outcrops form pods (on the order of 10 × 50 m) within a mafic schist that Nutman et al. (1984) termed the sequence A—lower amphibolite formation. Out of about 50 samples studied from several localities throughout the Isua belt, IW809-4 is the only one in which humite minerals were found, attesting to the relative rarity of these phases.

CHEMICAL COMPOSITION

Major elements

The major-element composition of sample IW809-4 was determined by microprobe analysis of glass prepared by fusion of 1.0 g each of sample powder and Li₂B₄O₇ flux using the same procedures applied to the analysis of the North American Shale Composite (NASC) by Gromet et al. (1984). Results are listed in Table 1 on a volatile-free basis and represent the weighted average of 15 replicate determinations.

The analysis shows the sample to be highly magnesian (Niggli value *mg* ≈ 0.9) with MgO, FeO, and SiO₂ being the only oxides present in amounts exceeding 1 wt%. [(Mg + Fe)/Si]_{atomic} is close to 2, and a cation-norm calculation yields an olivine content of ~95%. Thus, the bulk composition corresponds closely to a dunite. The small quantities of Na₂O, CaO, K₂O, and Al₂O₃ perhaps represent vestiges of accessory pyroxene, spinel, or mica originally present in the protolith, or they were added during metamorphism or alteration.

Loss-on-ignition (LOI) represents weight loss upon fusion for 15 min at 1000 °C on 1.0-g sample powder previously dried overnight at 110 °C. The value thus determined (~11 wt%) is quite high and indicative of the large amounts of serpentine and magnesite present in the sample (see below).

Trace elements

Abundances of V, Cr, Ni, Zn, Ga, Rb, Sr, Y, Zr, Nb, Ba, and Pb were determined by X-ray fluorescence anal-

ysis of pressed powder pellets at the University of Massachusetts, Amherst, using methods described in Rhodes et al. (1978). Tabulated results represent the average of analyses on two separate aliquants of the sample.

Values for most elements are very low, in several cases below practical limits of detection for the method employed. The high concentration of Ni (~2350 ppm) is consistent with the inferred original olivine-rich nature of the sample, whereas high Cr (~960 ppm) is probably due to spinel in the protolith. Of particular note is the high concentration of Pb (~13 ppm), which is contained in the rare sulfide mineral *shandite* (Dymek, 1987).

Rare-earth elements

Concentrations of eight REEs were determined by isotope-dilution mass spectrometry at Brown University using methods described in Gromet et al. (1984). A chondrite-normalized REE pattern (Fig. 1) reveals an unusual shape, with concave-down light REE, concave-up heavy REE, and a prominent negative Eu anomaly ($\text{Eu}/\text{Eu}^* = 0.376$).

This pattern shape is broadly similar to those reported for cumulate dunites of igneous origin, some of which have negative Eu anomalies (Fig. 1). The REE pattern shape of IW809-4 is also similar to that reported for a "soapstone" from the Tipasgarvi greenstone belt, Finland, which is also shown in Figure 1. Jahn et al. (1980) attributed the REE characteristics of the "soapstone" to alteration effects and suggested furthermore that such data provide no constraints whatsoever on the magmatic evolution of their sample.

PETROGRAPHY AND MINERAL CHEMISTRY

In thin section, the metadunite has a "spotted" appearance owing to the presence of large (several millimeters) subrounded areas that consist of relict olivine grains (or, less commonly, magnetite), which are surrounded and replaced to variable degrees by serpentine and magnetite. An example of the relict olivine is illustrated in Figure 2A, which consists of several polygonal cells that are separated from each other by fine magnetite dust.

These features correspond to what Wicks et al. (1977) have termed *mesh texture*. Thus, each polygonal cell contains an olivine core (*mesh center*) enclosed in platy, length-slow γ -serpentine (*mesh rim*). The individual mesh centers of olivine tend to extinguish simultaneously, indicating that they are segments of optically continuous single crystals. In some cases, an olivine mesh center is a multicrystal aggregate in which the individual crystals have rectangular to polygonal cross-sections.

Olivine

Olivine ranges from fuzzy and pale-brown to clear and colorless. Most of the olivine mesh centers consist of the fuzzy variety, and a spectrum of this material obtained with the laser Raman microprobe (LRM) reveals weak hy-

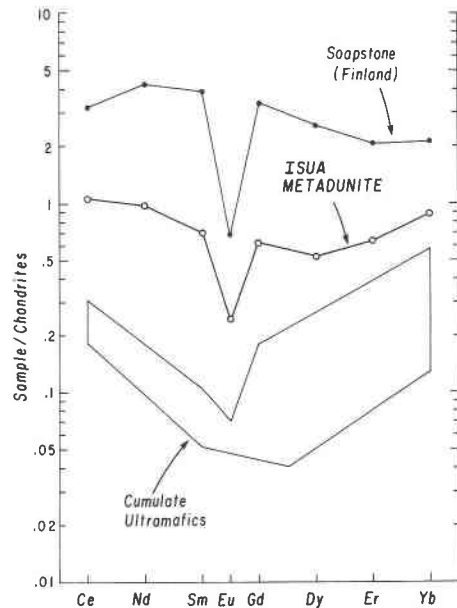


Fig. 1. Chondrite-normalized rare-earth-element pattern for Isua metadunite sample IW809-4. Also illustrated are data for a soapstone of similar bulk composition (from Jahn et al., 1980), and a field for ultramafic cumulate rocks—mostly of ophiolitic affinity (from Frey et al., 1971; Menzies, 1976; Montigny et al., 1973; Noiret et al., 1981; Pallister and Knight, 1981; Suen et al., 1979). All REE are normalized to the chondritic abundances of Nakamura (1974).

droxyl bands; perhaps incipient serpentinization is the cause of the fuzziness.

Finer-grained aggregates of the clear olivine surround many of the above-mentioned larger relict olivine grains. These crosscut the magnetite "dust" marking the relict grain boundaries, but are themselves replaced by (or simply intergrown with) elongate γ -serpentine (Fig. 2B). This crosscutting relationship suggests that clear olivine post-dates the fuzzy olivine.

Representative olivine analyses are listed in Table 2 (nos. 1 and 2). Both textural types are highly magnesian, but the clear variety is slightly more Mg rich (Fo_{98} vs. Fo_{97} ; Fig. 3). The high Fo content of these olivines is consistent with an origin through prograde metamorphism of serpentinite. This interpretation is supported by the fact that in all other analyzed Isua ultramafic rocks, $X_{\text{Mg}}^{\text{Ol}} \approx X_{\text{Mg}}^{\text{Rock}}$, whereas in IW809-4, $X_{\text{Mg}}^{\text{Ol}} > X_{\text{Mg}}^{\text{Rock}}$ (Dymek, unpub. results).

The abundance of minor elements are near or below limits of detection in both varieties of olivine, except for NiO and MnO, which range up to ~0.5 wt% each (Fig. 3). The fact that NiO exceeds MnO is somewhat unusual for metamorphic olivine, but most likely due to the absence of phases like talc, which tend to concentrate Ni compared to olivine (Evans, 1977).

Titanian humites

The identification of humite-group minerals was facilitated by their intense yellow color and pleochroism

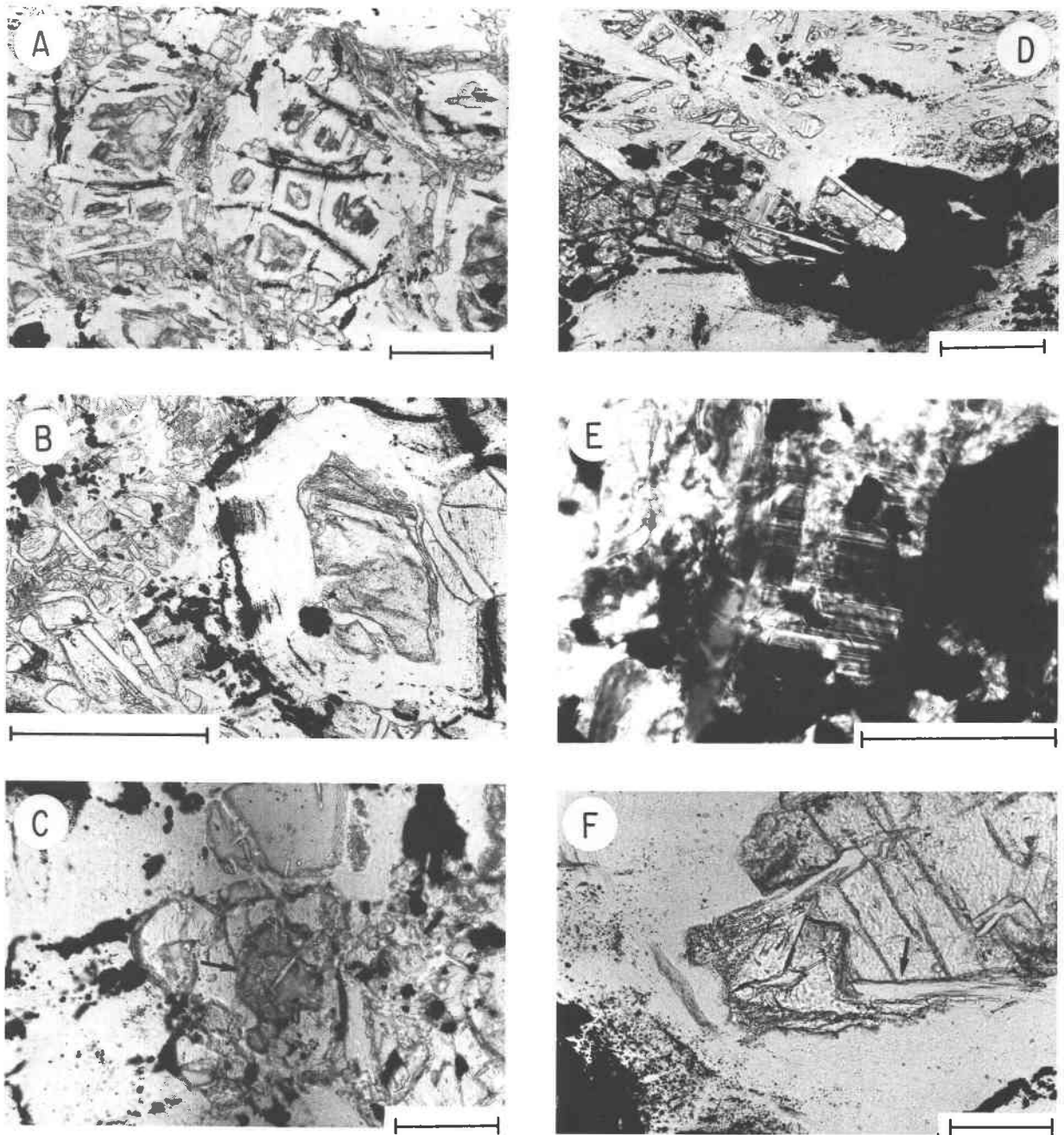


Fig. 2. Photomicrographs illustrating selected textural features of the metadunite. (A) Rounded, relict “fuzzy” olivine grain consisting of optically continuous polygonal subareas separated from each other by zones of platy serpentine and magnetite; arcuate clear olivine surrounds this grain at left center (transmitted, plane-polarized light; bar scale = 0.5 mm). (B) Relict “fuzzy” olivine (right of center) surrounded by platy serpentine. Note blocky magnetite (lower center) and clear olivine (left and far right); clear olivines are cut by elongate serpentine (transmitted plane-polarized light; bar scale = 0.5 mm). (C) Titanite chondrodite (rounded darker grain in center of field) enclosed in clear olivine (transmitted, plane-polarized light; bar scale = 0.1 mm). (D) Titanite chondrodite (high relief from left to center of field) intergrown with blocky magnetite, elongate serpentine and sulfide (large opaque in lower right). Note platy serpentine above sulfide and in lower left (transmitted, plane-polarized light; bar scale = 0.1 mm). (E) Lamellar structure in titanite chondrodite-clinohumite intergrowth (transmitted, cross-polarized light; bar scale = 0.1 mm). (F) Magnesite porphyroblast surrounded by platy serpentine and cut by elongate serpentine (arrow near center); the latter also cuts platy serpentine here (transmitted, plane-polarized light; bar scale = 0.1 mm).

TABLE 2. Representative analyses of olivine, serpentine, and magnetite from Isua metadunite IW809-4

	1	2	3	4	5
MgO	54.64	55.73	39.84	40.33	2.35
Al ₂ O ₃	0.00	0.00	1.21	0.41	0.00
SiO ₂	42.13	42.20	40.70	42.42	0.05
CaO	0.00	0.00	0.01	0.01	0.03
TiO ₂	0.00	0.00	0.06	0.02	0.00
V ₂ O ₅	—	—	—	—	0.02
Cr ₂ O ₃	0.02	0.03	0.12	0.11	0.27
MnO	0.28	0.29	0.00	0.01	0.11
FeO*	3.12	2.01	1.48	0.98	89.52
NiO	0.40	0.39	0.04	0.08	1.04
ZnO	—	—	0.01	0.00	0.08
Total (wt%)	100.59	100.65	83.46	84.35	93.47
Formula proportions					
Cations	3	3	10	10	3
Si	0.997	0.993	3.955	4.079	0.002
Ti	0.000	0.000	0.004	0.001	0.000
Al	0.000	0.000	0.138	0.046	0.000
Cr	0.000	0.000	0.010	0.008	0.008
Fe ³⁺	—	—	—	—	1.988
V	—	—	—	—	0.001
Mg	1.928	1.954	5.769	5.780	0.132
Fe ²⁺	0.062	0.040	0.120	0.079	0.831
Mn	0.006	0.006	0.000	0.001	0.003
Ni	0.008	0.007	0.003	0.006	0.032
Zn	—	—	0.000	0.000	0.002
Ca	0.000	0.000	0.001	0.001	0.001
X _{Mg}	0.969	0.980	0.980	0.987	0.137

Note: Columns are (1) olivine (fuzzy), (2) olivine (clear), (3) serpentine (platy), (4) serpentine (elongate), (5) magnetite (Calc. Fe₂O₃ = 70.15 wt%, FeO = 26.39 wt%, total = 100.50).

* Total Fe as FeO; formula proportions listed for Fe³⁺ and for Fe²⁺ apply only to magnetite.

(which resemble those of staurolite). Humite crystals are all xenoblastic and range in size from ~15 to 250 μm . They occur as inclusions in fuzzy olivine, as isolated masses surrounded principally by platy serpentine, or as complex intergrowths with magnetite, sulfide, and elongate serpentine (Figs. 2C, 2D, 2E). Most grains are optically homogeneous with inclined extinction, but a few show patchy coloration suggestive of compositional zoning. Other grains exhibit a distinct lamellar structure (Fig. 2E); analyses reveal these to be intergrowths of titanian chondrodite (Ti-Ch) and titanian clinohumite (Ti-Cl). Ti-Ch is by far the more abundant of the two humite-group minerals, whereas Ti-Cl occurs primarily in regions with lamellar structure. In one case, however, a thin partial rim of Ti-Cl occurs on Ti-Ch, where they are separated by an optical discontinuity.

As illustrated in Figure 4, the chondrodite phase contains variable TiO₂ (~8.5–10 wt%), and has a metal/Si ratio close to the ideal value of 2.50. The clinohumite phase also contains variable TiO₂ (~5.5–7.0 wt%), but has M/Si slightly above the ideal value of 2.25. This apparent departure from stoichiometry is most likely caused by the mode of occurrence of the Ti-Cl as thin lamellae. Backscattered-electron and X-ray imaging reveal streaking and heterogeneous Ti distribution parallel to lamellae orientation on a scale ranging from 10 μm down to the limits of practical resolution (ca. <2 μm). Accordingly, it

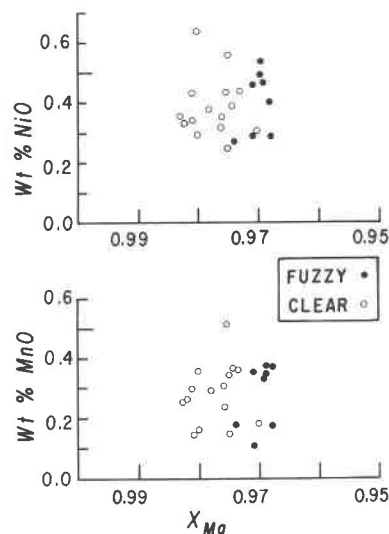


Fig. 3. Wt% NiO and MnO vs. X_{Mg} in olivine from metadunite IW809-4; note that "clear" olivine appears slightly more Mg rich than "fuzzy" olivine.

is probable that some of the Ti-Cl compositions are shifted slightly because of beam overlap with the host Ti-Ch phase during analysis.

Average compositions of the Ti-Ch and Ti-Cl are listed in Table 3. Both are highly magnesian ($X_{\text{Mg}} \approx 0.98$) with only small amounts of minor elements, principally MnO and NiO, and have low contents of F as well. Values for Fe/Mg, Ni/Mg, and Mn/Mg are essentially identical, but Ti/Mg and Ti/Si are clearly distinct (Table 4). The fact that Ti/Si in Ti-Ch is approximately double that in Ti-Cl supports the preferential substitution of Ti into the Mg(OH,F)O layer, as outlined by Ribbe (1979). The compositional characteristics of the Isua humites are considered in more general terms in the discussion section.

Serpentine

Serpentine forms platy masses, many of which are charged with extremely fine-grained particles of magne-

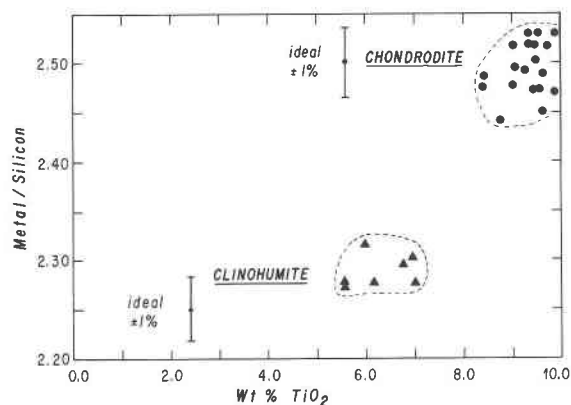


Fig. 4. Metal/Si vs. TiO₂ content in chondrodite and clinohumite from metadunite IW809-4.

TABLE 3. Compositions of titanian humites in Isua metadunite IW809-4

	1	2
MgO	50.55(0.46)	52.34(1.15)
Al ₂ O ₃	0.00(0.01)	0.02(0.03)
SiO ₂	33.96(0.45)	37.06(0.68)
CaO	0.00(0.00)	0.00(0.00)
TiO ₂	9.31(0.43)	6.18(0.65)
Cr ₂ O ₃	0.01(0.02)	0.02(0.02)
MnO	0.37(0.04)	0.35(0.02)
FeO	2.09(0.24)	1.99(0.21)
NiO	0.28(0.06)	0.35(0.08)
ZnO	0.01(0.01)	0.01(0.01)
F	0.28(0.06)	0.15(0.05)
Cl	0.00	0.00
H ₂ O*	2.84	1.34
-O≡F	99.70	99.81
	0.12	0.06
Total (wt%)	99.58	99.74
Formula proportions		
Cations	7	13
Si	2.007	3.949
Ti	0.415	0.495
Al	0.000	0.002
Cr	0.001	0.001
Mg	4.441	8.312
Fe	0.103	0.177
Ni	0.013	0.030
Mn	0.018	0.031
Zn	0.000	0.001
Ca	0.000	0.000
F	0.052	0.050
Cl	0.000	0.000
OH**	1.118	0.960
M/Si	2.495(0.026)	2.292(0.018)
X _{Mg}	0.977(0.003)	0.978(0.003)

Note: Columns are (1) chondrodite (average $\pm 1 \sigma$ for 19 analyses), (2) clinohumite (average $\pm 1 \sigma$ for 7 analyses).

* Calculated from anion proportions.

** Calculated from (2 - 2Ti - F - Cl).

TABLE 4. Selected cation ratios* for coexisting titanian humites in Isua metadunite IW809-4

	Chondrodite	Clinohumite
Fe/Mg	0.023 \pm 0.003	0.021 \pm 0.003
Ni/Mg	0.003 \pm 0.001	0.004 \pm 0.001
Mn/Mg	0.004 \pm 0.000	0.004 \pm 0.000
Ti/Mg	0.093 \pm 0.005	0.060 \pm 0.008
Ti/Si	0.206 \pm 0.011	0.125 \pm 0.015

* Data from Table 3.

ment substituents present in quantities significantly above detection limits are Cr₂O₃ and Al₂O₃, which range up to 0.3 wt% and 2.0 wt%, respectively. These analyses also demonstrate that platy serpentine is slightly but consistently more aluminous and less magnesian than the elongate type (Fig. 5). These differences perhaps could be caused by "contamination" of platy serpentine by the tiny magnetite inclusions, thus making them appear more Fe-rich. However, it is not possible to account for differences in Al content by this mechanism. Wicks and Plant (1979) also observed that serpentine plates from mesh rims after olivine contained Al₂O₃ (whereas precursor olivine has none).

Serpentine compositions are shown on a portion of the MgO-FeO-SiO₂ ternary diagram in Figure 6. The data points for platy serpentine cluster along the (Mg,Fe)₃Si₂O₅(OH)₄ join, whereas those for elongate serpentine plot on the SiO₂-rich side of this join. These compositional features, together with differences in Al contents noted above, suggest that platy serpentine is lizardite whereas elongate serpentine is antigorite (Wicks and Plant, 1979). Indeed, several investigators have determined that lizardite with a platy or banded texture is typical of serpentine mesh rims (Wicks and Whittaker, 1977).

The presence of antigorite in sample IW809-4 was confirmed by X-ray diffraction analysis (which also demonstrated the absence of brucite and chrysotile); however, the presence of lizardite could not be established. Similarly, the LRM spectrum of elongate serpentine matches almost perfectly that of an antigorite standard, whereas the LRM spectrum of platy serpentine is quite unlike that of a lizardite standard (but is virtually indistinguishable from the IW809-4 antigorite). The ability of the LRM to distinguish among the serpentine "polymorphs" is discussed by Pasteris and Wopenka (1987).

These conflicting results, whereby Mg/Si and Al content suggest the presence of both lizardite and antigorite but XRD and LRM indicate only antigorite, can be reconciled if the platy serpentine in IW809-4 crystallized originally as lizardite but "inverted" to antigorite during a later event during which the elongate antigorite formed. The fact that elongate serpentine cuts platy serpentine, as noted above, is consistent with this interpretation.

Magnesite

Magnesite forms large porphyroblasts, similar in size to the relict olivine grains, and is surrounded by platy

tite, locally concentrated in layers. These inclusions, along with flexing and/or bending (caused by positive ΔV during hydration of olivine?), impart a banded structure to the serpentine. This variety is found most commonly as pseudomorphs after olivine (Figs. 2A, 2B). Serpentine also occurs as ragged, elongate sheaths that crosscut the platy variety, and are also intergrown with the humites (Fig. 2D). The two types of serpentine are commonly found together (Fig. 2D), and the difference between them is not always so conspicuous.

Representative analyses of the two serpentine types are listed in Table 2 (nos. 3 and 4). Analytical totals are unfortunately low (by about 3–4 wt% from expected values near 87 wt%), a feature that appears in many published serpentine analyses (e.g., Cogulu and Laurent, 1984). This problem is symptomatic of all our analyses of Isua serpentines (Dymek, unpub. results), which we attribute to instability of serpentine under the electron beam even though a spot diameter of 20 μ m was used routinely.

The results, as such, yield very good formula proportions, and show that both serpentine compositions approach the pure Mg end member. The only minor ele-

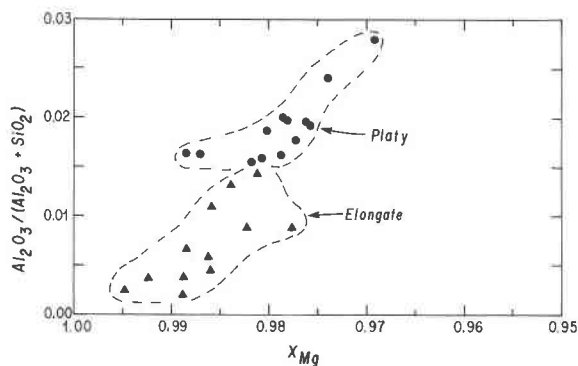


Fig. 5. Al/Si vs. X_{Mg} in serpentine from metadunite IW809-4 showing slight chemical differences between the platy and elongate varieties. The fact that the data points for each type are arranged in approximately parallel arrays of increasing Al/Si and decreasing Mg/Fe suggests a simple $Al_2Mg_{-1}Si_{-1}$ Tschermak-type substitution.

serpentine (Fig. 2F). Magnesite also occurs as smaller grains disseminated throughout the sample. It is highly likely that these smaller magnesites represent a second generation of carbonate.

Analyses show that the magnesite is nearly pure $MgCO_3$ ($X_{Mg} \approx 0.99$), with the following average composition (in wt%): MgO, 47.0; FeO, 0.80; MnO, 0.43; CaO, 0.08.

Magnetite

Magnetite occurs not only as the micrometer-sized "dust" associated intimately with serpentine, but also forms blocky grains (up to 50 μm across) that are found as inclusions within, or intergrown with, olivine, serpentine, humites, and sulfide (Figs. 2C, 2D, 2E). A representative analysis of blocky magnetite (Table 2, no. 5) shows that it contains little Cr_2O_3 , has essentially no detectable Al_2O_3 , V_2O_5 or TiO_2 , but has unusually high contents of MgO (2–3 wt%) and NiO (0.8–1.2 wt%). Such values are among the highest reported for a relatively pure Fe^{3+} spinel phase (cf., Haggerty, 1976). The high X_{Mg} is in line with the overall highly magnesian character of the silicates, whereas the elevated Ni content is most probably a result of the fractionation of that element into the magnetite during serpentinization of an originally Ni-bearing olivine [although it may also relate to reactions with nickel sulfides, as discussed in Dymek (1987)]. It was not feasible to obtain reliable analyses of the fine-grained magnetite.

Sulfides

Sulfides occur as somewhat amoeboid-shaped grains, up to 250 μm across, that are intergrown with clear olivine, titanian humites, magnetite and/or elongate serpentine (Figs. 2D, 2E). In addition, they are found as isolated masses (with magnetite) enclosed in platy serpentine. Each grain comprises composite aggregates of heazlewoodite (Ni_3S_2), cobalt pentlandite ($Co_7Ni_{15}Fe_{10}S_8$), and shandite

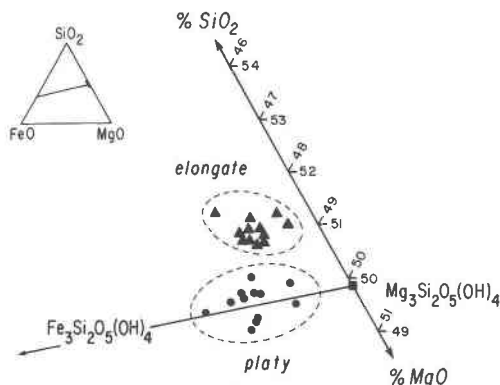


Fig. 6. A plot of normalized wt% MgO-FeO-SiO₂ in serpentine from metadunite IW809-4.

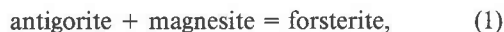
($Ni_3Pb_2S_2$), which are discussed in detail elsewhere (Dymek, 1987).

DISCUSSION

Metamorphic history

A multistage history for the metadunite is required by its complex petrography. We infer a magmatic stage, during which the primary dunite formed, followed by an episode of early serpentinization and carbonation, which is needed to account for the subsequent growth of very Mg-rich olivine during prograde metamorphism. This prograde event yielded fuzzy olivine, humites, blocky magnetite, magnesite, and sulfides. This was followed sequentially by formation of platy antigorite (i.e., the mesh texture), formation of clear olivine, and finally by later overgrowth of bladed antigorite (and additional magnesite?) on the other phases.

The bulk composition of the metadunite is approximated very closely by the model system $MgO-SiO_2-H_2O-CO_2$. In this system, Evans (1977) noted that the assemblage of forsterite + magnesite + antigorite lies along the univariant curve



at a pressure of 2000 bars and a temperature of ~ 450 – 480 °C for X_{CO_2} between 0.0 and 0.2 (Fig. 7). This temperature range is quite close to the estimate of ~ 470 °C for retrograde metamorphism of the Isua belt, as inferred from studies of pelitic assemblages (Boak and Dymek, 1982). The several stages of serpentinization and recrystallization could conceivably represent fluctuations in fluid composition and temperature, such that Reaction 1 has been crossed at least twice, to form two separate generations of olivine, magnesite, and antigorite.

As shown in Figure 7, Reaction 1 intersects an invariant point involving talc. Throughout the Isua belt, talc + magnesite \pm antigorite schist is ubiquitous as the retrograde product of metaperidotite. However, talc is not found in sample IW809-4, which is problematic: either it never formed or else it was eliminated completely by later reactions.

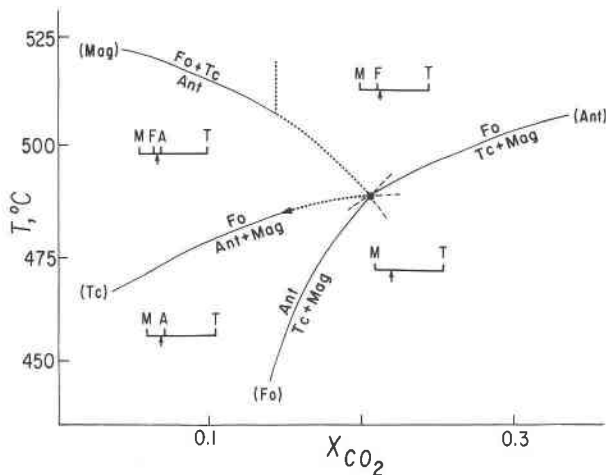


Fig. 7. T - X_{CO_2} diagram showing the relationship among the phases forsterite (Fo), magnesite (Mg), antigorite (Ant), and talc (Tc). [Adapted from Evans, 1977; see text for discussion.] The arrow shows the bulk composition of the Isua metadunite along the join magnesite-talc.

The latter interpretation seems more consistent with regional geologic relationships. Early prograde metamorphism of the ultramafic rocks produced assemblages with magnesiocummingtonite and/or anthophyllite (Brothers and Dymek, 1983), which are above the stability of antigorite. For the bulk composition of IW809-4 (shown by the arrows in Fig. 7), talc would have appeared above reaction (Mag), albeit in small amounts. Subsequent retrograde metamorphism probably followed a T - X_{CO_2} path such as shown by the dashed line in Figure 7, which would have eliminated talc and produced the observed assemblage of forsterite + magnesite + antigorite.

Regardless of such speculations, the fact that titanian chondrodite occurs as inclusions in fuzzy olivine suggests that it formed relatively early in the evolution of this sample. Thus, the "late" history of IW809-4 places no limitations on the P - T regime in which the humite phase originally crystallized—a regime that was most likely above the stability of antigorite based on the overall character of the Isua ultramafic rocks, as noted above. Hence, even though Trommsdorff and Evans (1980) offered convincing evidence that the stability of hydroxyl Ti-Cl is restricted to antigorite metaperidotite, the same conclusion need not apply to Ti-Ch. We consider this point in more detail in a later section.

Comparison with other titanian humites

Compositions of titanian humites, compiled from a variety of sources, are summarized on Figures 8 and 9. In both diagrams, the tie lines connect the compositions of intergrown Ti-Cl and Ti-Ch reported by Aoki et al. (1976; cf. Fujino and Takéuchi, 1978).

The other analyses of Ti-Cl yield M/Si ratios that scatter about the ideal value of 2.25 (Fig. 8); perhaps those three compositions with the highest M/Si contain humite

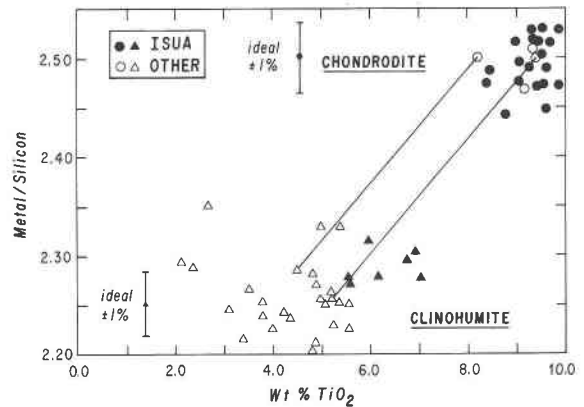


Fig. 8. Metal/Si vs. TiO_2 content in Isua titanian humites compared to other occurrences (sources listed in Fig. 10); tie lines connect compositions of intergrown chondrodite-clinohumite reported by Aoki et al. (1976).

intergrowths that have yet to be recognized. The few other analyses of Ti-Ch have M/Si very close to the ideal value of 2.50. X_{Mg} in the other samples spans a wide range of values (~ 0.84 – 0.96), which in all cases are more Fe-rich than the Isua humites (Fig. 9). The Ti-Ch and Ti-Cl pair from Aoki et al. (1976) show similar values for X_{Mg} , as do the Isua data. In terms of TiO_2 content, the analyses of Isua Ti-Cl are slightly but consistently more Ti-rich than the other occurrences, whereas the Isua Ti-Ch are also slightly more Ti-rich (on average) than the others. Collectively, these data and comparisons reveal how close the Isua humites are to the ideal end-member compositions for Ti-Cl and Ti-Ch, $Mg_8Si_4O_{15}(OH) \cdot Mg_{0.5}Ti_{0.5}O_2$ and $Mg_4Si_2O_7(OH) \cdot Mg_{0.5}Ti_{0.5}O_2$, respectively.

Trommsdorff and Evans (1980) have remarked upon the general absence of Fe-Mg fractionation between coexisting titanian humites and olivine, which is supported by our results. Figure 10 summarizes data on olivine-humite pairs; with the exception of two occurrences (one of which is Mn-rich), the data indeed fall close to the line (K_D)Fe-Mg = 1.0. For the Isua humites, equal Fe-Mg partitioning is best for the clear olivine.

Some comments on Ti in the humites

The humite minerals constitute a homologous or polysomatic series that has been considered traditionally as combinations of olivine and brucite (or sellaite) groups having the general formula $n(Mg_2SiO_4) \cdot Mg(OH,F)_2$ ($n = 1$, norbergite; $n = 2$, chondrodite; $n = 3$, humite; $n = 4$, clinohumite). Ribbe et al. (1968) pointed out that such groups, in fact, do not exist and have no structural significance and that it would be more appropriate to regard, for example, the norbergite formula as $Mg_2SiO_3(OH,F) \cdot Mg(OH,F)O$. The various members of the humite series can thus be viewed as stacked, ordered sequences of norbergite and forsterite modules, as discussed by Thompson (1978).

Each member of the humite series has a correspond-

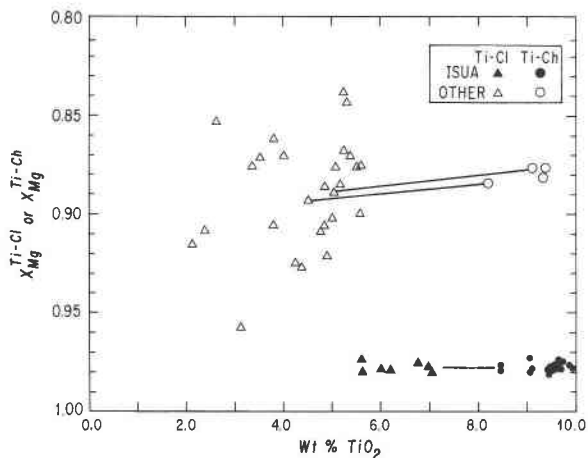


Fig. 9. X_{Mg} vs. TiO_2 content in Isua titanian humites compared to other occurrences (sources listed in Fig. 10). Note that the Isua analyses are more magnesian than all others and that there is no significant Fe/Mg fractionation between the Ti-Ch and Ti-Cl.

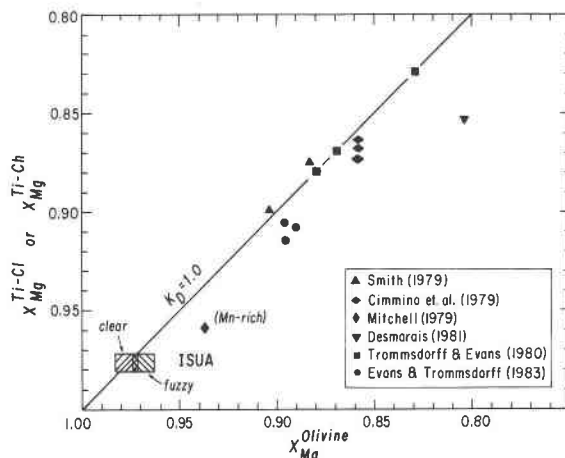


Fig. 10. X_{Mg} in coexisting olivine and titanian humite. As noted by Trommsdorff and Evans (1980), most pairs lie near the $K_D = 1.0$ line, although there is a slight tendency for olivine to be more Fe-rich.

ing Ti-rich variety described by the general formula $[(n - 1)Mg_2SiO_4][Mg_2SiO_3(OH,F) \cdot Mg_{1-x}Ti_x(OH,F)_{1-2x}O_{1+2x}]$, in which X cannot exceed 0.5 (Ribbe, 1979). Compositional variations in titanian humites can be portrayed by means of a simplified model chemical system (Evans and Trommsdorff, 1983) defined by three linearly independent exchange vectors: (1) $FeMg_{-1}$, (2) $F(OH)_{-1}$, and (3) $TiO_2Mg_{-1}(OH)_{-2}$; an additional exchange, (4) $TiO_2Mg_{-1}F_{-2}$, is an alternative to exchange 3. This model system, condensed along $FeMg_{-1}$, is shown in Figure 11. In order to examine relationships among Ti, F, and (OH) substitutions, it is useful to transform this ternary to a binary diagram in which the axes, X_{Ti} (= Ti cations/formula) and X_F (= 0.5 F anions/formula), are the measurable parameters of interest (see Fig. 12). On such a diagram, exchange 2 operates vertically, exchange 3 operates horizontally, and exchange 4, which is actually a linear combination of 2 and 3, is represented by a 45° line.

Jones et al. (1969) first evaluated Ti and F contents of the humite minerals. Their analyses (not plotted) scatter in the area below and to the left of the 45° line in Figure 12, indicating no general relationship between Ti and F. Evans and Trommsdorff (1983), however, drew attention to the fact that their analyses of Alpine Ti-Cl formed a linear array that plotted very close to the 45° line (Fig. 12), thus indicating a strong coupling of Ti with F. They argued that such evidence for internal (crystal-chemical) control on exchanges 2 and 3 was apparent only in closely related specimens.

Analyses of Isua Ti-Cl extend this array to still lower values of F. Analyses of Isua Ti-Ch, however, plot below the 45° line and form an approximate horizontal array. This suggests (assuming negligible contributions from analytical error) that the two humites behave somewhat differently; because Ti substitution occurs on the same por-

tions of the chondrodite and clinohumite structures (i.e., exclusively within the norbergite module), it is difficult to account for these findings solely in terms of crystal chemistry. As discussed in the next section, the differences between the two Isua humites may reflect variable $P-T$ conditions of their formation.

Petrogenesis of the titanian humites

Trommsdorff and Evans (1980) observed that the breakdown of Ti-Cl in the Alpine peridotites is marked by the appearance of geikielite ($MgTiO_3$). One might expect that the breakdown of Ti-Ch would likewise involve a geikielite-forming reaction. We have searched for this mineral at great length but have failed to find it. The apparent absence of geikielite suggests that the thermal stability of the titanian humites has not been approached and additional possibilities should be explored. For ex-

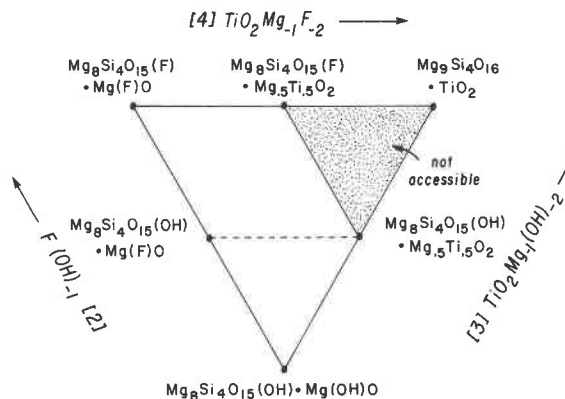


Fig. 11. Model chemical system for the humite minerals (condensed on $MgFe_{-1}$). Although this diagram is drawn for clinohumite, identical relationships apply for other members of the series (adapted from Evans and Trommsdorff, 1983).

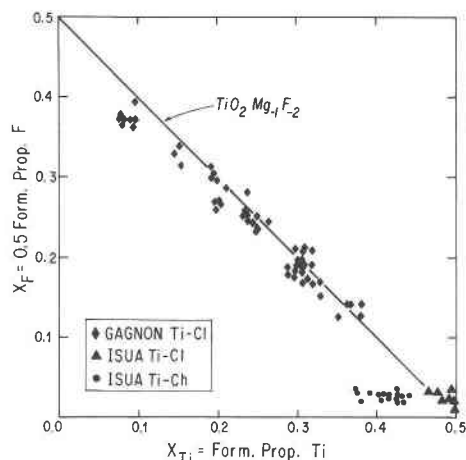


Fig. 12. A plot of X_F (= 0.5 F anions/formula) vs. X_{Ti} (= Ti cations/formula) for titanian humites. Data for Ti-Cl fall near the 45° line, closely approximating $TiO_2Mg_{-1}F_{-2}$ exchange, whereas data for Ti-Ch plot below this line (see text for additional discussion). Note that Evans and Trommsdorff (1983, p. 361) stated that their Fig. 3, from which the present one is adapted, uses $X_F = [F/(F + OH)]$ as a plotting parameter. When X_F is defined this way, the dashed line in Fig. 11 maps as a curve in the above figure; however, data points in their Fig. 3 were plotted (correctly) using X_F as defined herein (B. W. Evans, pers. comm.).

ample, Hinz and Kunth (1960) have determined that, in the system Mg_2SiO_4 - MgF_2 , clinohumite breaks down to chondrodite + forsterite. The lack of F and the presence of high Ti contents in the Isua humites preclude direct application of these experimental results. Nevertheless, the general idea of a humite series "reaction relationship" may provide insight into the interpretation of our observations.

The compositions of the Isua humites are contained almost completely in the ternary system Mg_2SiO_4 - $MgTiO_3$ - H_2O (see Fig. 13) in which the following four univariant reactions characterize relevant phase relations:

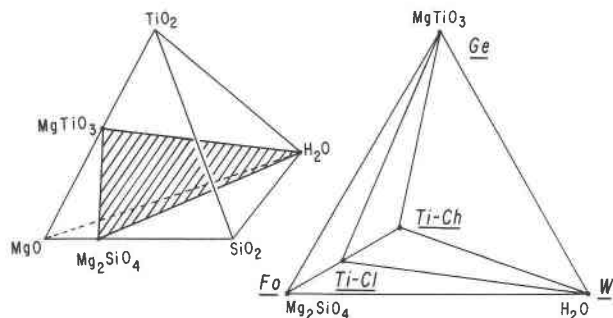


Fig. 13. The quaternary system MgO - SiO_2 - TiO_2 - H_2O , showing the plane Mg_2SiO_4 - $MgTiO_3$ - H_2O (Fo-Ge-W) that describes the compositions of end member Ti-Ch and Ti-Cl; the four univariant reactions in the ternary subsystem are shown in Fig. 14.

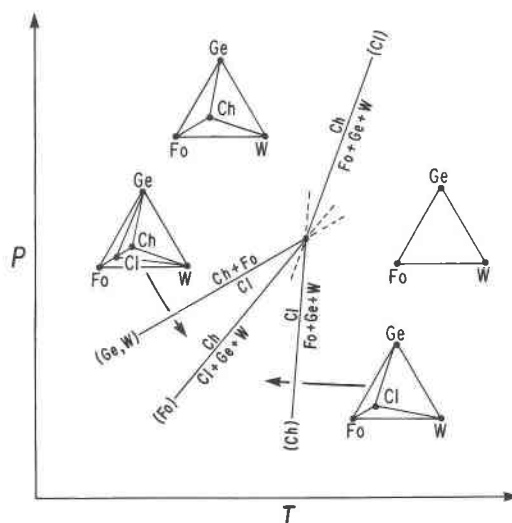
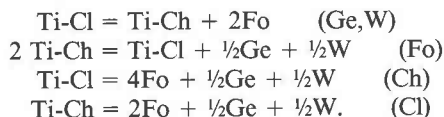


Fig. 14. Schematic P - T orientation for the four univariant reactions in the ternary subsystem Fo-Ge-W (H_2O). Intergrowths of Ti-Cl and Ti-Ch and the total absence of geikelite may indicate conditions between the reactions (Ge,W) and (Fo) (see text for discussion).



The P - T orientation of these reactions is shown schematically in Figure 14. Because reaction (Ch), which represents the terminal breakdown of Ti-Cl, has been shown through experiment to have a very steep positive slope (Engi and Lindsley, 1980), the other reactions are required topologically to have Ti-Ch on the high-pressure side. Of particular significance to our interpretations is the vapor-absent reaction (Ge,W), which represents the formation of Ti-Cl from Ti-Ch + Fo.

Because of the general lack of thermodynamic data for the titanian humites, calculated slopes for these reactions are uncertain. Nevertheless, applying the Clapeyron relationship to the data compiled by Duffy and Greenwood (1979) indicates $dP/dT \approx 2.5$ kbar/100 K for (Ge,W) in the Ti-free system, with $\Delta V_R = 9.6$ cal·kbar $^{-1}$. Engi and Lindsley (1980) reported $\Delta V_R = 12 \pm 3$ cal·kbar $^{-1}$ for (Ge,W) in the Ti system. Unless there are drastic, unexpected differences in ΔS_R for the Ti-rich system compared to the Ti-free system, dP/dT for (Ge,W) should be similar to the value listed above. Where (Ge,W) intersects (Ch) is unknown, but it should be at high pressure ($T \approx 600$ °C, $P \approx 25$ kbar), as Engi and Lindsley (1980) have synthesized Ti-Ch from Ti-Cl + Ge at $T = 600$ °C, $P = 23$ kbar (this synthesis should lie between the reactions (Fo) and (Ge,W) shown in Fig. 14).

Although there are clearly large uncertainties in this analysis of the titanian humites, the important point regarding the reaction topology of Figure 14 is that the two-phase intergrowths of Ti-Ch and Ti-Cl found here (and

in the kimberlite by Aoki et al., 1976) may represent an arrested "decompression" reaction. Accordingly, Ti-Ch ought to be evaluated further as a possible upper-mantle mineral, as it is the expected high-pressure phase. Information on other occurrences of titanian humites and experimental data on the stability of Ti-Ch are needed to resolve this issue.

In regard to the Isua sample, we do not consider this metadunite to be of mantle origin, as there is no petrologic or geochemical evidence among the suite of ultramafic rocks to warrant such a conclusion. It does appear, however, that its metamorphic *P-T-t* trajectory passed through a "higher pressure" region where Ti-Ch was stable and that later retrogression caused the Ti-Ch to react partly to Ti-Cl.

ACKNOWLEDGMENTS

Funding for this project was provided by grants from the National Science Foundation (EAR78-23412 and EAR81-09466) and the National Aeronautics and Space Administration (NAGW-484 and NAG9-98; Early Crustal Genesis Program). Additional support for field work at Isua was provided by a grant from the National Geographic Society.

We thank J. Sparks, University of Massachusetts, Amherst, for assistance in obtaining the X-ray fluorescence analyses, and L. P. Gromet, Brown University, for use of his laboratory for the rare-earth-element determinations. We also thank the Department of Geological Sciences, Harvard University, for permission to use their microprobe laboratory, while we were in residence there.

Comments on an earlier version of this manuscript by H. W. Day, C. A. Francis, and L. P. Gromet helped to clarify and focus our presentation, and their efforts are most appreciated. Finally, journal reviews by B. W. Evans and M. Engi resulted in considerable improvement of the paper. J. D. Pasteris, Washington University, kindly obtained the laser Raman microprobe spectra on the serpentines and olivine. We thank Freda Sofian for typing the manuscript.

REFERENCES CITED

- Allaart, J.H. (1976) The pre-3760 m.y. old supracrustal rocks of the Isua area, central West Greenland, and the associated occurrence of quartz-banded ironstone. In B.F. Windley, Ed., *The early history of the Earth*, p. 177-189. Wiley, New York.
- Aoki, K., Fujino, K., and Akaogi, M. (1976) Titanochondrodite and titanoclinohumite derived from the upper mantle in the Buell Park kimberlite, Arizona, USA. *Contributions to Mineralogy and Petrology*, 56, 243-253.
- Baadsgaard, H., Nutman, A.P., Bridgwater, D., Rosing, M., McGregor, V.R., and Allaart, J.H. (1984) The zircon geochronology of the Akilia association and the Isua supracrustal belt. *Earth and Planetary Science Letters*, 68, 221-228.
- Boak, J.L., and Dymek, R.F. (1982) Metamorphism of the ca. 3800 Ma supracrustal rocks at Isua, West Greenland: Implications for early Archaean crustal evolution. *Earth and Planetary Science Letters*, 59, 155-176.
- Bridgwater, D., and McGregor, V.R. (1974) Field work on the very early Precambrian rocks of the Isua area. *Rapports Grønlands geologiske Undersøgelse*, 65, 49-54.
- Brothers, S., and Dymek, R.F. (1983) Ultramafic metamorphic rocks from the 3800 Ma Isua supracrustal belt, West Greenland. *Geological Society of America Abstracts with Programs*, 15, 534.
- Cimmino, F., Messiga, B., Piccardo, G.B., and Zeda, O. (1979) Titanian clinohumite-bearing assemblages within antigoritic serpentinite of the Voltri massif (western Liguria): Inferences on the geodynamic evolution of Piemontese ultramafic sections. *Ofoliti*, 4, 97-120.
- Cogulu, E., and Laurent, P. (1984) Mineralogical and chemical variations in chrysotile veins and peridotite host-rocks from the asbestos belt of southern Quebec. *Canadian Mineralogist*, 22, 173-183.
- Desmarais, N.R. (1981) Metamorphosed Precambrian ultramafic rocks in the Ruby Range, Montana. *Precambrian Research*, 16, 67-101.
- Duffy, C.L., and Greenwood, H.J. (1979) Phase equilibria in the system MgO-MgF₂-SiO₂-H₂O. *American Mineralogist*, 64, 1156-1172.
- Dymek, R.F. (1987) An occurrence of shandite, Ni₃Pb₂S₂, in a serpentinized metadunite from the Isua supracrustal belt, West Greenland. *Canadian Mineralogist*, 25, 245-249.
- Dymek, R.F., Boak, J.L., and Brothers, S. (1983) Ti-chondrodite (Ti-Ch) and Ti-clinohumite (Ti-Cl) in ca. 3800 Ma metadunite from Isua, West Greenland (abs.). *EOS*, 64, 327.
- Engi, M., and Lindsley, D.H. (1980) Stability of titanian clinohumite: Experiments and thermodynamic analysis. *Contributions to Mineralogy and Petrology*, 72, 415-424.
- Evans, B.W. (1977) Metamorphism of Alpine peridotite and serpentinite. *Annual Reviews of Earth and Planetary Science*, 5, 397-447.
- Evans, B.W., and Trommsdorff, V. (1983) Fluorine hydroxyl titanian clinohumite in Alpine recrystallized garnet peridotite: Compositional controls and petrologic significance. *American Journal of Science*, 283-A (Orville volume), 355-369.
- Frey, F.A., Haskin, L.A., and Haskin, M.A. (1971) Rare earth abundances in some ultramafic rocks. *Journal of Geophysical Research*, 76, 2057-2070.
- Fujino, K., and Takéuchi, Y. (1978) Crystal chemistry of titanian chondrodite and titanian clinohumite of high-pressure origin. *American Mineralogist*, 63, 535-543.
- Gromet, L.P., Dymek, R.F., Haskin, L.A., and Korotev, R.L. (1984) The "North American Shale Composite" (NASC): Its compilation, major and trace element composition. *Geochimica et Cosmochimica Acta*, 48, 2419-2482.
- Haggerty, S.E. (1976) Opaque minerals in terrestrial igneous rocks. *Mineralogical Society of America Reviews in Mineralogy*, 3, H6101-H6300.
- Hinz, W., and Kunth, P.O. (1960) Phase equilibrium data for the system MgO-MgF₂-SiO₂. *American Mineralogist*, 45, 1198-1210.
- Jahn, B.M., Suvray, B., Blais, S., Capdevila, R., Cornichet, J., Vidal, F., and Hameurt, J. (1980) Trace element geochemistry and petrogenesis of Finnish greenstone belts. *Journal of Petrology*, 21, 201-244.
- Jones, N.W., Ribbe, P.H., and Gibbs, G.V. (1969) Crystal chemistry of the humite minerals. *American Mineralogist*, 54, 391-411.
- McGetchin, T.R., Silver, L.T., and Chodos, A.A. (1970) Titanoclinohumite: A possible mineralogical site for water in the upper mantle. *Journal of Geophysical Research*, 75, 255-259.
- Menzies, M. (1976) Rare earth geochemistry of fused ophiolitic and alpine lherzolites, I. Othris, Lanzo and Troodos. *Geochimica et Cosmochimica Acta*, 40, 645-656.
- Mitchell, R.H. (1979) Manganous magnesium ilmenite and titanian clinohumite from the Jacupiranga carbonatite, Sao Paulo, Brazil. *American Mineralogist*, 63, 544-547.
- Montigny, R., Bougault, H., Bottinga, Y., and Allègre, C.J. (1973) Trace element geochemistry and genesis of the Pindos ophiolite suite. *Geochimica et Cosmochimica Acta*, 37, 2135-2147.
- Nakamura, N. (1974) Determination of REE, Ba, Fe, Mg, Na and K in carbonaceous and ordinary chondrites. *Geochimica et Cosmochimica Acta*, 38, 757-775.
- Noiret, G., Montigny, R., and Allègre, C.J. (1981) Is the Vourinos Complex an island arc ophiolite? *Earth and Planetary Science Letters*, 56, 375-386.
- Nutman, A.P., Allaart, J.H., Bridgwater, D., Dimroth, E., and Rosing, M. (1984) Stratigraphic and geochemical evidence for the depositional environment of the early Archaean Isua supracrustal belt, southern West Greenland. *Precambrian Research*, 25, 365-396.
- O'Leary, E.F., and Dymek, R.F. (1987) Biopyrite in Archaean ultramafic rocks, West Greenland (abs.). *EOS*, 68, 452.
- Pallister, J.S., and Knight, R.J. (1981) Rare-earth element geochemistry of the Samail ophiolite near Ibra, Oman. *Journal of Geophysical Research*, 86, 2673-2697.
- Pasteris, J.D., and Wopenka, B. (1987) Use of a laser Raman microprobe to trace geological reactions. In R.H. Geiss, Ed., *Microbeam analysis—1987*, 205-209.
- Rhodes, J.M., Blanchard, D.P., Dungan, M.A., Rodgers, K.V., and Brannon, J.C. (1978) Chemistry of Leg 45 basalts. In W.G. Melson et al., Eds., *Initial reports of the Deep Sea Drilling Project*, 45, 447-459.

- Ribbe, P.H. (1979) Titanium, fluorine and hydroxyl in the humite minerals. *American Mineralogist*, 64, 1027–1035.
- Ribbe, P.H., Gibbs, G.V., and Jones, N.W. (1968) Cation and anion substitutions in the humite minerals. *Mineralogical Magazine*, 37, 966–975.
- Smith, D. (1977) Titanochondrodite and titanoclinohumite derived from the upper mantle in the Buell Park kimberlite, Arizona, USA: Discussion. *Contributions to Mineralogy and Petrology*, 61, 213–215.
- (1979) Hydrous minerals and carbonates in peridotite inclusions from the Green Knobs and Buell Park kimberlitic diatremes on the Colorado Plateau. In F.R. Boyd and H.O.A. Meyer, Eds., *The mantle sample: Inclusions in kimberlites and other volcanics*, vol. 2, p. 345–356. American Geophysical Union, Washington, D.C.
- Suen, C.T., Frey, F.A., and Malpas, J. (1979) Bay of Islands ophiolite suite, Newfoundland: Petrologic and geochemical characteristics with emphasis on rare earth element geochemistry. *Earth and Planetary Science Letters*, 45, 337–348.
- Thompson, J.B., Jr. (1978) Biopyriboles and polysomatic series. *American Mineralogist*, 63, 239–249.
- Trommsdorff, V., and Evans, B.W. (1980) Titanian hydroxylclinohumite: Formation and breakdown in antigorite rocks (Malenco, Italy). *Contributions to Mineralogy and Petrology*, 72, 229–242.
- Wicks, F.J., and Plant, A.G. (1979) Electron-microprobe and X-ray-microbeam studies of serpentine textures. *Canadian Mineralogist*, 17, 785–830.
- Wicks, F.J., and Whittaker, E.J.W. (1977) Serpentine textures and serpentinization. *Canadian Mineralogist*, 15, 459–488.
- Wicks, F.J., Whittaker, E.J.W., and Zussman, J. (1977) An idealized model for serpentine textures after olivine. *Canadian Mineralogist*, 15, 446–458.

MANUSCRIPT RECEIVED AUGUST 8, 1986

MANUSCRIPT ACCEPTED JANUARY 20, 1988